sustainability

MDPI

Article

The Passivhaus Standard in the Spanish Mediterranean: Evaluation of a House's Thermal Behaviour of Enclosures and Airtightness

Víctor Echarri-Iribarren [1,*], Cristina Sotos-Solano [1], Almudena Espinosa-Fernández [2] and Raúl Prado-Govea [1]

[1] Department of Building Construction, University of Alicante, Carretera de San Vicente s/n, San Vicente del Raspeig, 03690 Alicante, Spain

[2] Department of Architecture, University of Zaragoza, Calle María de Luna, 3, 50018 Zaragoza, Spain

* Correspondence: Victor.Echarri@ua.es; Tel.: +34-965-903677

Received: 3 June 2019; Accepted: 4 July 2019; Published: 8 July 2019

Abstract: Few houses have been built in the Spanish Mediterranean in accordance with the Passivhaus (PH) standard. This standard is adapted to the continental climates of Central Europe and thorough studies are necessary to apply this standard in Spain, especially in the summer. High relative air humidity levels in coastal areas and solar radiation levels of west-facing façades require adapted architectural designs, as well as greater control of air renewal and dehumidification. A priori, energy consumptions undergo big variations. In this study, the construction of a single-family house in the Spanish Levante was analysed. All enclosure layers were monitored using sensors of surface temperature, solar radiation, indoor and outdoor air temperature, relative humidity, and air speed. The thermal behaviour of the façade enclosure and air infiltration through the enclosure were examined using the blower door test and impacts on annual energy demand were quantified. Using simulation tools, improvements are proposed, and the results are compared with examples of PH housing in other geographical areas. The annual energy demand of PH housing was 69.19% below the usual value for buildings in the Mediterranean region. Very thick thermal insulation and low values of airtightness could be applied to the envelope, which would work very well in the winter. These technique solutions could provide optimal comfort conditions with a well-designed air conditioning system in summer and low energy consumption.

Keywords: Passivhaus; thermal transmittance of enclosures; air infiltration; annual energy demand; energy efficiency

1. Introduction

Within the European Union, the energy consumption of buildings represents 40% of final energy consumption. Buildings are responsible for 36% of CO_2 emissions. A total of 85% of the energy consumed is used to heat or cool rooms, illuminate them, and heat sanitary water. In December 2002, the European Parliament approved the Energy Performance Building Directive, EPBD 2002/91/EC, with the aim of improving energy efficiency [1]. Long-term strategies have been established to decrease energy consumption and to reduce CO_2 emissions, based on the Kyoto Protocol. Both exterior and local weather conditions are taken into account, as well as internal climatic conditions and the cost-effectiveness ratio. A few years later, a revised text was approved, Directive 2010/31/EU, known as the EPDB Recast [2]. Thus, the regulations on Nearly Zero Energy Buildings, known as NZEBs, were introduced for all new buildings from year 2020 onwards [3]. This text was revised in 2012 and has now become Directive 2012/27/EU [4].

All European Union member states made the commitment to submit themselves to the same directive and the 2020 goal is shared. However, the way of implementing the regulatory framework is defined by each country individually. Each country also individually establishes the criteria to assess buildings' energy efficiency and the needs of buildings with almost zero energy consumption. As the specific way of applying the EPDB is thus dispersed, not all countries situate themselves within the same ranges of energy consumption and CO_2 emissions, which is added to the fact that the energy efficiency evaluation criteria also differ.

Spain, as a member of the European Union, is today undergoing an 'energy transition'. The country is currently implanting renewable energy and energy efficiency in the national electricity system. The ultimate objective is to reshape the energy sector so that renewable energies account for 20% of final gross energy consumption in 2020 and 27% by 2030, with a possible increase of 30%. Spain's legislative framework regulating the energy efficiency of buildings consists in the Technical Building Code (or CTE by its Spanish acronym) [5]. This code came into effect in 2006 and was modified in 2009 [6], 2010, and more substantially in 2013 [7], to comply with the European Union's successive guidelines. A major change introduced in 2013 is the reduction of the maximum thermal transmittance *U* value allowed in a building envelope's elements. Heating and cooling energy consumption has also been restricted. In addition, types of climate according to the building's location and user profiles have been defined, both for residential and non-residential buildings. Currently, a new modification is underway whereby the energy efficiency strategies of the EU's building guidelines will be approved for nearly zero energy consumption buildings.

1.1. The Passivhaus Standard

A variety of standards define the requirements that buildings must comply with to guarantee minimum energy efficiency values. The most widespread is the Passivhaus (PH) standard. It was developed in Central European countries and the European Union uses the requirements found within it as design principles for energy efficient buildings [8].

The key PH standard requirements are as follows:

1. Annual heating demand must not exceed 15 kWh/m^2;
2. Annual demand for primary energy for heating, electricity and DHW must be less than or equal to 120 Kwh/m^2;
3. The volume of filtered air should not be greater than 0.6 air changes per hour (ACH), measured with a pressure of 50 Pa, as verified by an on-site test using the Blower Door test.

Further requirements were added to apply the standard to warmer climates, as follows:

4. Annual cooling demand must not exceed 15 kWh/m^2;
5. Thermal comfort must be achieved in all rooms of the house throughout the year. Therefore, the regulation allows 10% of indoor air temperature overheating, representing 10% of the total hours of a complete one-year cycle above 25 °C.

The main problem when adapting buildings on the Mediterranean coast to the PH standard is that in northern and central European countries, energy demands focus exclusively on heating. In southern Europe, however, air conditioning or cooling needs must be taken into account in summer, in addition to heating demands in winter. It is also worth noting that a large part of the population lives on the coast, with high relative humidity values, and buildings require high dehumidification values of outdoor renewal air, with its corresponding increase in energy demand in summer [9]. For this reason, a large amount of research and development projects focus on adapting homes with passive systems in warmer climatic conditions [10], in which these techniques are combined with PH standard requirements. Some of the most relevant projects are as follows:

CEPHEUS project: Study of more than 100 homes in five northern European countries [11]. Low levels of energy consumption were obtained, while occupants' thermal comfort remained optimal [12].

Passive-On project [13]: It focused on implementing the PH concept in southern European climates. The passive house concept was found to be viable, provided essential prior studies are conducted to adapt and detail the technical and constructive solutions in each specific region [14].

MED-ENEC: Different procedures were implemented through demonstration projects to show how to solve construction sector challenges in the southern Mediterranean region [15].

IEEA project: It addresses the passive strategies that could be adopted in different climatic zones of the EU [16].

ECO-BÂT project: Promoted by local authorities in Algeria [17]. It focuses on low-cost passive strategies and on affordable active measures that use renewable energy technologies.

Southern European passive houses: It was found that a pleasant indoor climate could be achieved by preconditioning the ventilation system's supply air [18]. Night ventilation has the same effect as façade insulation, especially when applying a mechanical ventilation system equipped with a by-pass.

Due to its successful implementation in Central Europe, the PH standard has been applied in other geographical and climatic zones, such as the Spanish Mediterranean region. In this sense, housing design under the Mediterranean climate must take into account parameters such as building orientation, solar gains in winter, thermal insulation of the envelope with a high thermal capacity, windows with double or triple glazing, solar control, control of thermal bridges to minimise them, both fixed and mobile solar protections, cantilevers, ventilation and natural lighting, etc. In addition, air renewal installations with double flow heat recovery systems must be improved.

The state-of-the-art regarding PH standard implementation provides interesting results that help determine its applicability in climates such as that of the Mediterranean coast. Figueiredo et al., after analysing a single-family, two-storey, 148 m^2 detached house of light construction in the region of Aveiro (Portugal), concluded that the problem of overheating of indoor air and walls constituted the main obstacle to achieving the PH standard in Portugal [19]. They emphasised the need to use a shading and solar protection system, in addition to increasing the enclosures' thermal inertia, thus attenuating thermal wave oscillation of the interior air temperature T_i. Costanzo, Fabbri, and Piraccini studied a house in Cesena (Italy) and concluded that its design, drawn up using the Passive Housing Planning Package (PHPP), was able to guarantee suitable comfort conditions during the heating period [20]. However, on the other hand, overheating during the cooling season was recorded for almost 50% of the time, according to the EN 15251 standard [21], an excessively high value. This value could be reduced to 20% by reducing the insulating material thickness (up to one third of the original value) on the roof and walls, replacing triple glazed windows with double glazed windows, and implementing a hybrid ventilation strategy instead of using mechanical ventilation with heat recovery (MVHR). Suárez, Prieto, and Salgado studied a house on the northern coast of Spain [22]. If the house were to be renovated, installing a ventilation system with heat recovery, improving the insulation of opaque building elements, replacing existing windows with high thermal efficiency windows, and reducing air infiltration rates to below 0.6 ACH, the annual energy demand would be below that required by the PH standard and the heating and cooling needs would be respectively reduced by 81% and 57% of the current values. With regard to the coast of Catalonia (Spain), Pesic, Roset, and Muros proposed the methodology "Climate potential for natural ventilation" (CPNV). They achieved notable cooling energy savings by applying a mixed mode (or hybrid mode) and night ventilation techniques [23], which could be used to achieve, along with other construction techniques in the installations, the PH standard. This same line was adopted by Fokaides et al. in Cyprus, when they studied a house in Nicosia with 110 m^2 of usable floor area. The nocturnal natural ventilation significantly reduced summer period overheating, making it possible to comply with the EN 15251 standard. Users must be sufficiently trained to adapt their behaviour to the home's thermal needs [24]. The application of the standard in Algeria throws some light on the issue. Ali-Toudert and Weidhaus concluded that night and day ventilation of 4 ACH was needed. The energy demand in winter was low, with a maximum value of 5.5 kWh/m^2yr, while in summer it was higher, with 9.7 kWh/m^2yr [25]. Other studies in climates with less hot summers focus on the use of passive and active systems [26], such as Mihai et al. in Bucharest, with earth-to-air heat exchange technology (EAHX) with photovoltaic panels, generating 1,556.5 kWh/year, and a drop in annual energy demand to 13 kWh/m^2yr [27]. Harkouss, Fardoun, and Biwole, through multi-criteria decision making (MCDM), further refined the technical quantification of thermal insulation and thermal transmittance U values in warm climates at 0.6 W/m^2K for walls, 0.6 W/m^2K for ceilings, and 0.5 W/m^2K for floors [28]. In mixed climates, the walls and ceiling should be well insulated (U= 0.2 W/m^2K), while the floor's thermal transmittance should not be minimised so as to allow the heat to escape through the floor in summer. A low window/surface area ratio value (10%) is necessary to improve buildings' energy performance.

From this review of the state-of-the-art, we can conclude that, to date, few PH dwellings have been built on the Spanish Mediterranean coast. Some of the research has focused on applying bioclimatic techniques in order to comply with the PH standard and to improve climatic conditions in summer, while others have limited themselves to quantifying energy demand in summer and winter. However, the absence of more detailed quantifications, according to the different parameters and intervening agents, of the energy consumption produced in these PH dwellings is detected. The novelty of this research is the quantification of energy consumption due to the transmission of heat through the various elements of the enclosures and of the actual infiltration of air through the enclosure by means of the analysis of a representative PH case study.

1.2. Aims and Objectives

The present study examined the implementation of the Passivhaus standard in the Spanish Mediterranean. It focused on the impact that building envelope heat flows and air infiltration have on annual energy demand [29]. To this end, the construction of an isolated detached house in Molina de Segura (Spain), located 40 km away from Spain's Eastern coast was studied. The house was designed with the aim of complying with the Passivhaus standard. The façade enclosures were monitored and thermal transmittance measurements were made in situ. The Blower Door air infiltration test was also conducted. Subsequently, using the Design Builder simulation tool [30], results on the quantification of the impact on energy demand were obtained for both parameters, both in the studied house and in the hypothetical case that it would have been built in the city of Alicante, on the coast [18]. Since the standard was designed to improve energy efficiency under a continental climate, the intention was to draw a conclusion on whether the standard could also be appropriate for coastal climate situations. Relative air humidity in the months of summer and autumn is much higher than that experienced in Central European countries, as well as wall and indoor air overheating by solar gains through glazing [31]. The thermal gaps between indoor air temperature and outdoor air temperature during the winter and spring months are more moderate. These big differences call into question, a priori, the validity of initial investments in the construction quality and the control devices for air renewal installations with heat recovery.

In addition to the tests mentioned previously, we proceeded to evaluate the parameters selected in this study in other houses in the area, according to local construction culture. First, we examined houses built before 1979 (without thermal insulation), then buildings built after the NBE CT-79 standard came into force [32], and finally, buildings constructed after 2006, after the CTE was implemented [5]. The enclosures of the latter buildings are resolved using two sheets with an air chamber and 6 cm of thermal insulation, an inverted flat roof with 6 cm of thermal insulation finished with gravel, and air permeable class 2 joineries (27 m^3/hm^2), with silicone-based sealing and double hollow brick walls, and high air infiltration standards according to the n_{50} index. In this way, results obtained in the present study can be compared with other construction systems and installations, allowing further studies to conclude on the suitability of the Passivhaus (PH) standard for Spanish Mediterranean coast buildings.

2. Description of the Case Study

The isolated detached house under study is located in Molina de Segura (Spain), 40 km from the coast (Figure 1). It is composed of two volumes. The lower volume has day areas (living room, laundry room, pantry, toilet, and office) and a floor area of 100 m^2. The first floor corresponds to the night area (3 bedrooms, 2 bathrooms, and a study) and has a constructed surface area of 95 m^2. There are covered porches on the outside with a constructed area of 43 m^2, which help to protect the house from solar radiation, resulting in a total floor area of 216.15 m^2. The bedrooms are south-facing to capture the largest possible amount of solar radiation in winter, while the living room and kitchen face a north-south axis, obtaining an axis of natural ventilation that passes through the house. Overheating in summer can thus be avoided (Figure 2). The gaps in the exterior façade have been planned in such a way as to capture a maximum amount of natural light. Overhangs and solar protections based on adjustable blades were designed to avoid direct solar radiation in summer. Flat roofs with small punctual overhangs protect the gaps from the impact of sunlight in summer.

Figure 1. View of the southeast façade. Main access to the house.

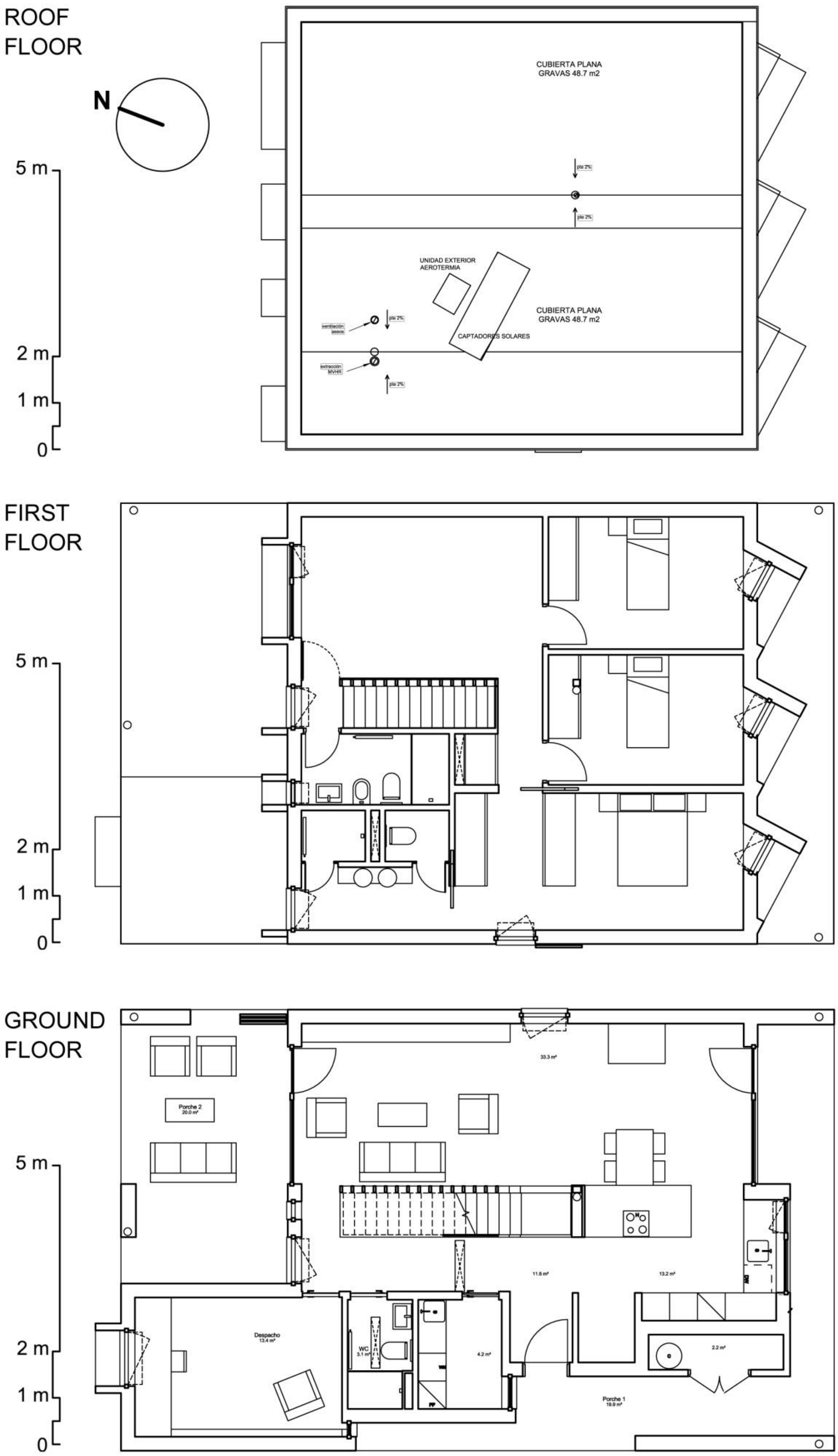

Figure 2. Floors of the house.

The façade on the ground floor is resolved with a thermal insulation system on the outside (SATE), thus constituting a ventilated façade made with a stucco lime mortar coating with flexible silicate on vertically modulated 32 × 100 mm mullions, a waterproof EPDM sheet, 15 mm Superpan Tech board, on a structure of modulated wooden posts every 60 cm and filled with natural 160 mm mineral wool, Micro USB barrier 230/20 Riwega, and laminated wood board on a self-supporting 73 × 48 structure (Figure 3). On the first floor, the exterior enclosure is a ventilated façade formed by larch wood slats, a 32 × 100 mm ventilation strip, Riwega waterproof sheet, 15 mm Superpan Tech board on a structure of modulated wooden mullions every 60 cm and filled with 148 mm natural mineral wool, and Micro USB 230/20 Riwega vapour barrier, with laminated wood board on a 73 × 48 self-supporting structure (Figure 4). All joineries between elements are solved with an adhesive tape seal, Riwega USB Tape 1 PE (60mm wide, professional and universal polyethylene with mesh reinforcement coated with high adhesive strength acrylic adhesive), which guarantees perfect air-tightness (Figure 5), as later verified with the results of the Blower Door test. The joinery is made of wood with thermal bridge break, elastic joint, Guardian-Sun type laminated glass (6 + 16 + 3 + 3), and Guardian-Sun type glass (6 + 16 + 4) for the non-laminated glazing.

Figure 3. View of the southeast façade. Construction of enclosures and floors.

The roof is flat, not passable, and is made with slopes, a SuperPan Tech P5 21 mm board, 200 gr/m^2 geotextile separating layer plus EPDM membrane waterproofing 1 mm thick, and a finishing layer of 5 cm-thick clean gravel, on a 198 × 48 wooden beam structure, 2 SuperPan Tech P4 25 mm wooden boards containing a 200 mm natural mineral wool thermal insulation layer, and a continuous suspended ceiling with a metal structure, formed by a laminated plaster plate. The foundation is based on a reinforced concrete slab, with a thermal insulation of XPS, 100 mm thick, and an EPDM waterproofing sheet, as well as self-levelling mortar and a class 3 microcement pavement.

Figure 4. Wooden structure and Superpan Tech 15 mm board partitions with 148 mm mineral wool thermal insulation.

The house has a low-temperature solar collector system for domestic hot water demand (DHW), in addition to auxiliary aerothermal equipment [33], located in the laundry room, which intervenes when there is insufficient solar radiation collection. In addition to natural ventilation, mechanical ventilation was installed with heat recovery with a contribution of 5 l/s per person in the bedrooms, 2 l/s per person in the living and dining rooms, and 2 l/s per m^2 in the kitchen, as specified in the CTE-DB-HS3. One air conditioning system is included, coupled to the ventilation system, and composed of an exterior machine as well as an indoor one, with a direct expansion cold-only air-air system. The EER value is 5.93 and the COP is 4.27.

Figure 5. Lacquered aluminium carpentry joined to the exterior pavement. Airproof sealing and waterproofing with EPDM (left). Interior partitions and enclosure with tape sealing, type Riwega USB Tape 1 PE (right).

2.1. Climatic and Normative Conditions

The house location is under a Mediterranean climate. According to the Köpen–Geiger classification [34], it is classified as BSh, a warm semi-arid climate with hot or very hot summers and mild winters with very little rainfall [35]. The average annual temperature is 18.1 °C, the coldest month being January, with an average of 10.3 °C, and the hottest month being August, with an average of 26.3 °C.

According to the Spanish regulations in force at the time of building the CTE house (2013 modification), it is located in a B3 climatic zone with an altitude of 240 m above sea level, letter B in winter and 3 in summer, according to the CTE-DB-HE table B1 classification (Climate Zones).

2.2. Energy Demands Obtained in the Project Phase

According to the current calculation procedure in Spain, CTE DB-HE-2013, using the Unified Tool Lider-Calener (HULC), the demand for renewable energy consumption was 29.7 kWh/m^2·year. The annual heating demand was 6.41 kWh/m^2·year, below the demand level required by the CTE (26.29 kW·h/m^2·year). Cooling energy demand was 4.17 kWh/m^2·year, i.e., below that required by the CTE (15 kWh/m^2·year).

3. Materials and Methods

The two domains of evaluation of the house's energy demand are linked to the materials used as well as the technical characteristics of the enclosures, although they are of a very different nature. Evaluating the actual heat flow through the enclosures throughout the year's entire cycle is a complex matter [36]. This evaluation requires simulation models that take into account construction faults, the impact of thermal inertia, real thermal bridges, as well as the incidence of solar radiation on the exterior surfaces and the air conditioning systems used. Air infiltration through the enclosures varies according to the external environment's climatic conditions, the air pressure at each moment, as well as how occupants maintain and use certain mobile elements such as joinery, adjustable slats, or grids. All this means that estimating the energy impact due to air infiltration is complex.

3.1. U Thermal Transmittance of the Enclosures

Fourier's law, which applies to parallel layers of materials, of an unlimited surface, in steady state indoor T_i and exterior T_e air temperatures, establishes the temperature gradient reached by multi-layer enclosures when there is a thermal gap between outdoor and indoor air temperatures (Equation (1)). Thermal transmission by conduction and convection intervene according to values of resistance to the passage of heat or superficial thermal resistance due to the convection currents generated.

$$U - value = \frac{1}{R_T} = \frac{1}{\frac{1}{h_i} + \sum_0^n \frac{e_i}{\lambda_i} + \frac{1}{h_e}}. \quad (1)$$

However, this law is valid only for ideal situations and steady states. Walls have limited surfaces, they present discontinuities due to joineries and glazing, thermal bridges due to construction faults [37,38], etc. In addition, the various layers are made up of different types of materials with different values of physical parameters of resistance to the passage of the heat [39]. Furthermore, outdoor air conditions are altered by solar radiation, air speed, water vapour pressure in the air, etc. Solar radiation also often has an impact on the outer surfaces, substantially increasing their temperature. Indoors, thermal loads and the air conditioning systems used alter the physical parameters of interior air temperature and relative humidity, as well as the surface temperatures of the walls [40]. Finally, the thermal inertia of the materials making up the enclosure alters the linear Fourier process as a function of time, since the thermal gap between exterior and interior air temperature, the solar radiation that affects the exterior surface, or the interior air conditioning systems vary according to the weather. Heat flow thus becomes a dynamic and complex process [41].

3.1.1. Theoretical Calculation of the U Transmittances of the Enclosures

In this study, we measured the house's thermal transmittance *U* value, but we did not analyse the effect of the parameters affecting the dynamic regime of the heat flow through the enclosures, such as thermal admittance, *Y*, and thermal wave lag [42], *df*, or the damping factor of the thermal wave, f_a. The thermal transmittance *U* values were obtained according to the method established by the current regulations, the Technical Building Code (CTE) [43].

The usual values of thermal conductivity, λ, of the materials used in the enclosure, according to UNE EN ISO 10456: 2012 [44,45], were compared to the measurements obtained from real samples by means of the thermal conductivity analyser C-Therm TCi by Mathis Instrumentos Ltd., using a universal sensor, made at the University of Alicante. We proceeded with a theoretical calculation of the heat flow resistance of the enclosure's different layers, under ideal conditions, according to Fourier's law.

To simulate this behaviour in a steady state, we overlooked the impact of other energy sources, such as solar radiation, the indoor conditioning system, or the effect of material effusiveness or thermal inertia [46], and decided to apply the maximum outdoor air temperature in summer (39.57 °C) and the minimum outdoor temperature in winter (7.87 °C), collected by PT 100 monitoring sensors, and an indoor air temperature of 28.62 °C in summer and 17.74 °C in winter, without the air conditioning system operating. To do this, we considered, in accordance with the CTE [47], that surface thermal resistance was $1/h_i$ of 0.13 m^2 K/W, surface thermal resistance was $1/h_e$ of 0.04 m^2 K/W, and thermal resistance, R_c, of the ventilated façade chamber was 0.0176 m^2 K/W.

3.1.2. In-Situ Measurements of U Transmittance

Subsequently, a thermoflumetric study of the opaque enclosures was conducted to measure *U* thermal transmittance [48,49]. It was measured in the two rooms on the southeast façade (the kitchen at a height of 0.70 m and the dining room), in the northwest façade (the living room), as well as in the bedrooms on the first floor in the northeast and southwest façades. For this, the ISO 9869-1: 2014 [50] standard was followed. The equipment consisted of a heat flow plate; a transducer that generates an electrical signal proportional to the total heat rate applied to the sensor surface. Two indoor and outdoor air temperature probes were attached to this plate, as well as two surface temperature sensors for the exterior and interior surfaces. These were connected to the analyser directly with cables or through the window. The trial lasted one week for each of the three measurements. The data was analysed using the module that calculates thermal transmittance, part of the AMR WinControl software developed by Ahlborn for ALMEMO measuring equipment. The method used was the "average method", which assumes that thermal transmittance or thermal conductivity can be calculated by dividing the average density of the thermal flow by the average temperature difference [51].

This analysis was completed with the thermal imaging and detection of possible thermal bridges, helping to determine the outer envelope's ventilated chamber behaviour [52,53], though quantifying thermal bridges was not the subject of this study [54].

3.2. Air Infiltration Through the Envelope

The air infiltration value through the enclosure was forecast to be very low thanks to the construction's quality, the seals used, and the joinery quality. It was evaluated by means of the Blower Door test conducted in accordance with the European Standard EN 13829, using the Blower Door GMBH MessSysteme für Luftdichtheit equipment. The corresponding graphs were obtained and there was an n_{50} air infiltration value of 50 Pa. To characterise the information obtained, the Minneapolis Blower Door Model 3 software (TEC-TITE 5.0) was used. This tool was developed specifically to describe 140 parameters that possibly intervene in the filtration phenomenon [55]. These parameters were collected in a database used to perform a general evaluation of the results.

To obtain the average value of air infiltration in the building, a parameter difficult to quantify, and to be able to perform the energy impact simulations using the Design Builder tool, thus obtaining the values of annual energy demand, the protocol established in the UNE-EN-ISO 13790: 2003 standard was followed, which it allows for converting the value of n_{50} to renewals/hour under normal pressure conditions by means of Equation (2):

$$n_{winter} = 2 \cdot n_{50} \cdot e_i \cdot \varepsilon_{\mathrm{i}} \qquad (2)$$

where:

n_{50} renewals/hour at 50 pascals;
e_i wind protection coefficient = 0.05; and
ε_{i} height corrector factor = 1.

The Blower Door test was the tool used to detect thermal bridges through images using a ThermaCam P 25 thermographic camera from Flyr. It was quantified using the AnTherm program. Load losses or gains due to thermal bridges were estimated at 3.5% of the total thermal loads by *U* thermal transmittance of the enclosures. These values are similar to values obtained in previous studies [56,57].

3.3. Energy Impact Assessment

As mentioned, the main objective of the present study was to quantify the energetic impact of the heat flow through the envelope and air infiltration. Both values were obtained using different tools and methodologies.

3.3.1. Energy Losses due to U Transmittance Values

To quantify the energetic impact, the transmittance *U* values of all the enclosures obtained in-situ were introduced into the Design Builder tool. To perform building behaviour simulations in terms of energy demand and interior comfort parameters, the data and parameter values that follow were introduced into the Design Builder tool. The winter period covered 1 December to 30 April and the summer period covered from 1 May to 30 November. This decision was based on results from previous studies, contrasted with the experience of various calibrations of models in the same geographical location. The interior air setpoint temperatures were 21 °C in winter and 24 °C in summer. For the standard calculation of air renewal, occupancy was 5 people. To comply with regulations, a value of 0.63 air changes per hour (ACH) of air renewal was established, in accordance with the Technical Building Code (CTE) currently in force. The air infiltration values introduced in the tool were those obtained from the Blower Door test. Table 1 shows the parameters introduced in Design Builder's simulation model.

Table 1. Summary of parameters introduced in Design Builder's simulation model.

Parameter	Data Introduced
Hours of operation and occupancy: Monday to Friday: 7 am to 3 pm	25 % occupancy
Hours of operation and occupancy: Monday to Friday: 3 pm to 8 pm	50 % occupancy
Hours of operation and occupancy: Monday to Friday: 8 pm to 7 am	100 % occupancy
Hours of operation, activity and occupancy: Saturday and Sunday	100 % occupancy
Climate equipment operating hours (heating)	7 am to 10 pm
Climate equipment operating hours (cooling)	9 am to 8 pm
Running of the air conditioning system from Monday to Sunday	7 days/week
Summer period	1 May to 30 November
Winter period	1 December to 30 April
Occupancy density (5 people)	0.03 person/m^2
Metabolic factor: "Standing/walking" option	1.20
Clothing values (CLO)	Winter CLO = 1.00 Summer CLO = 0.50
Load due to general lighting	300 lux
Internal air temperature setpoint *Ti* (cooling)	24 °C
Set internal air temperature *Ti* (heating)	21 °C
Indoor air maintenance temperature *Ti* (cooling)	26 °C
Internal air maintenance temperature *Ti* (heating)	18 °C
Relative humidity of the indoor air	50%
Air renewal rate	0.63 acH
Air infiltration through the envelope	0,049 acH

3.3.2. Annual Energy Demand due to Air Infiltration

Estimating the air infiltration's energy impact is a complex issue. It depends not only on the sealing of the building envelope, but also on weather conditions, which are sometimes very difficult to predict. No common criterion exists regarding the right model to evaluate the energetic impact of infiltrations. Until now, different calculation models have been developed with varying degrees of complexity and reliability. The simplest models presuppose a uniform distribution of leak paths and average constant leaks over time. In the present study, this impact was evaluated using a simplified model (Equation (3)), applying the concept of degree-day, which relates the average temperature outside the house under study and the interior comfort temperature (21 °C for heating and 24 °C for cooling) [7]. This estimate is theoretical and actual energy consumption depends on the particular conditions of the houses' internal air temperature setpoint, T_i. This calculation procedure allows evaluating the energetic impact, taking into account the climatic data specific to the area around the house. The air infiltration flow, specific air capacity, and the air temperature difference between the interior and the exterior of the house were all taken into consideration [58].

$$Q_{inf} = C_p \cdot G_t \cdot V_{inf}, \quad (3)$$

where:

Q_{inf} is annual energy loss (kWh/yr) due to air infiltration for heating $Q_{inf\text{-}H}$ and cooling $Q_{inf\text{-}C}$·;
C_p is the air's specific heat capacity, which is 0.34 Wh/m^{3}K;
G_t are annual degrees-days (kKh/yr); and
V_{inf} is the air leak rate (m^3/h).

The Persily–Kronvall estimate is simple and the model is widespread in the scientific community [59]. It assumes a linear relationship between permeability at 50 Pa and average annual infiltration (Equation (4)).

$$q_{inf} = q_{50}/20, \quad (4)$$

where q_{inf} is the air permeability (m^3/(h m^2)).

Subsequently, this linear relationship between leakage and infiltration evolved [59] and incorporated coefficients according to the characteristics of the location of the Equations (5) and (6).

$$q_{inf} = q_{50}/\mathrm{N}, \quad (5)$$

$$\mathrm{N} = \mathrm{C} \cdot cf_1 \cdot cf_2 \cdot cf_3, \quad (6)$$

where:

N is a constant;
C is the climatic factor;
cf_1 is the building's height correction factor, 1 (cf_1 = 1) to 3 (cf_1 = 0.7) floors;
cf_2 is the site screening correction factor, for well shielded cases (cf_2 = 1,2), (cf_2 = 1) (cf_2 = 1) or exposed dwellings (cf_2 = 0.9); and
cf_3 is the sealing correction factor, which depends on the value of the exponent of leak n.

This simplified extended model has been adopted to calculate the average infiltration flow in Spain's Mediterranean area, obtaining the value of climatic factor C via equivalence with US climates, based on average temperature and wind speed. For the coefficients cf_1, cf_2, and cf_3, a value equal to 1 was adopted in all three cases. The type of infiltration opening was obtained from the mean value of the flow exponent n = 0.59. The V_{inf} air leak rate, necessary to calculate the energy impact, was calculated based on the air permeability rate and the envelope surface area, as follows (Equation (7)):

$$V_{inf} = q_{inf} \cdot A_E, \quad (7)$$

where A_E is the envelope area.

Once the value of the volume of air infiltration through the envelope or air leak rate V_{inf} was obtained to calculate the energetic impact, according to the annual average corrected by means of equations (3–7), sensible and latent heats were quantified by means of the following Equations (8) and (9):

$$Q_s = V_{inf} \cdot C_e \cdot \rho \cdot (T_e - T_i), \quad (8)$$

where:

Q_s is the energy impact value of the sensible heat of the air leak rate V_{inf} (W);
V_{inf} is the air leak rate (m^3/h);

C_e is the specific heat of the air under normal conditions 0.349 Wh/kgK;
ρ is the density of air (kg/m^3);
T_e is the outside air temperature in degrees Kelvin (K), considered as the average annual value; and
T_i is the air temperature inside the house (21 °C in winter and 24 °C in summer).

$$Q_l = V_{inf} \cdot C_v \cdot \rho \cdot (W_e - W_i), \tag{9}$$

where:

Q_l is the energetic impact value of the latent heat of the air leak rate V_{inf} (W);
C_v is the heat of water vaporization (0.628 W/g$_{vapour}$);
W_e is the specific humidity of the external air taken as the annual average value (g$_{vapour}$/kg);
W_i is the specific humidity of the indoor air (g$_{vapour}$/kg).

4. Results

The measurements of some thermal behaviour parameters of the materials used in the house's enclosures are presented in Table 2. They do not differ substantially from those obtained in other similar publications [40]. In this way, the thermal transmittance *U* values of a typical enclosure, according to Fourier or in steady state, were obtained following the values of surface thermal resistance and air chambers established by the CTE.

Table 2. Thermal conductivity values according to UNE EN ISO 10456:2012 and measurements using Mathis TCi equipment.

Materials of the Enclosure Layers	Thickness *e* (cm)	Thermal Conductivity λ W/m K	Thermal Conductivity λ Mathis TCi
Multilayer coating Coteterm + Calcifin	0.5	1.21	0.27
Hollow ceramic brick	11.5	0.49	0.52
SuperPan Tech P5 water-repellent wood panel	1.5	0.76	0.75
Thermal isolation. Mineral wool	14.8	0.038	0.0334
Thermal isolation. Purone mineral wool 35 QN	19.8	0.038	0.0361
Riwega USB Tape 1 PE adhesive tape	0.05	0.17	0.183
Class 3 microcement pavement	2.0	1.38	1.392
Pieces of 90 x 60 cm porcelain stoneware	1.0	2.30	2.21
Polished concrete	3.0	1.63	1.652

With these values, we proceeded to make a theoretical calculation according to Fourier and λ values extracted from the UNE EN ISO 10456: 2012 standard, of the *U* thermal transmittances of conventional enclosures. Table 3 shows the calculation for the opaque enclosure.

Table 3. *U* value of thermal transmittance for the opaque enclosure according to λ values extracted from the standard UNE EN ISO 10456:2012, established in the CTE.

Vertical Enclosure and Horizontal Flow		Thermal Resistance		
LAYERS		Thickness	λ	R
		[m]	[W/m·K]	[m^2·K/W]
1	Exterior environment (Rse)			0.040
2	Multilayer coating Coteterm + Calcifin	0.005	1.21	0.004
3	SuperPan Tech P5 water-repellent wood panel	0.015	0.14	0.107
4	Thermal isolation. Mineral wool type IV	0.148	0.0334	4.428
5	SuperPan Tech P5 water-repellent wood panel	0.015	0.14	0.107
6	Interior environment (Rsi)			0.130
R_T = Sum R_i [m^2·K/W]				4.816
U_T = 1/R_T [W/(m^2·K)]				0.2075

The U thermal transmittance measurements made using the sensors and Testo equipment (Figure 6) are shown in Table 4, together with the comparison of the theoretical calculation results in a steady state [36]. As shown, deviations ranging between 1% and 7% were detected. They are also compared with the usual measurement results of enclosures in standard building types in the Spanish Mediterranean area over the periods 1979–2006 and 2006–2019 [60].

Figure 6. Measurement of U thermal transmittance of the opaque house enclosure; 11 April 2019, 5 pm.

Table 4. Value of the U thermal transmittance according to λ values extracted from the standard UNE EN ISO 10456:2012 and according to measurements made using Testo equipment. Comparison with other usual constructions.

	Passivhaus House		Standard House	
	U Value W/m^{2}K	U Value Testo Equipment W/m^{2}K	1979–2006 Period U Value W/m^{2}K	2006–2019 Period U Value W/m^{2}K
Opaque	0.207	0.221	0.476	0.421
Glazing	2.910	2.932	3.520	3.450
Roof	0.208	0.210	0.508	0.458
Ground	0.325	0.307	0.485	0.465

Regarding the air infiltration values from the Blower Door test, carried out in two phases dated 21 June 2018 and 3 October 2018 (Figure 7), the results are shown in Table 5. As can be seen, the average value is 0.51 air changes per hour (ACH) at 50 Pa, a lower value than the maximum allowed by the PH standard (Figure 8). In comparison with the values obtained for other buildings in the area, and in other geographical parts of Spain, the value is significantly lower. It is between 600% and 1200% below that of isolated single-family homes in the area built between 1979 and 2019, whose n_{50} values are between 3 and 6 ACH [61].

Table 5. Values of air infiltration through the envelope at 50 Pa. PH house compared to standard housing types in the Murcia-Alicante area.

	Passivhaus House		Standard House	
Valor n_{50} (ACH)	**Blower Door Test 1 21 June 2018**	**Blower Door Test 2 3 October 2018**	**1979–2006 Period**	**2006–2019 Period**
Depressurization	0.35	0.51	6.52	3.69
Pressurization	0.33	0.48	6.05	3.43
Average value (ACH)	0.34	0.49	6.23	3.56

Figure 7. Image during the Blower Door test; 3 October 2018.

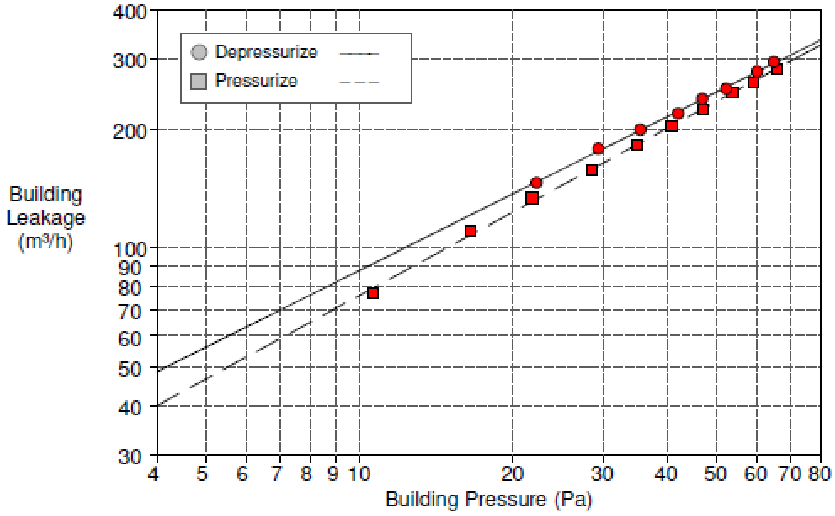

Figure 8. Results of the Blower Door test; 3 October 2018.

4.1. Energetic Impact of Heat Flow Through the Envelope

Once we obtained the enclosures' *U* values of thermal transmittance, the values of indoor air renewal rate according to CTE, air infiltration through the envelope, surface temperatures of the walls, house occupancy, etc., we proceeded to simulate the house's thermal behaviour using the Design Builder tool (Figure 9) [29]. It was thus possible to analyse users' feeling of comfort, the temperature gradients in the rooms, and to compare the summer and winter energy demands depending on the characteristics of the enclosures and the Blower Door test. Simulations could also be made by modifying the technical characteristics of the enclosures [62], modifying the air infiltration rate factor n_{50}, and other parameters [42]. As indicated, the interior air setpoint temperatures applied were 21 °C in winter and 24 °C in summer.

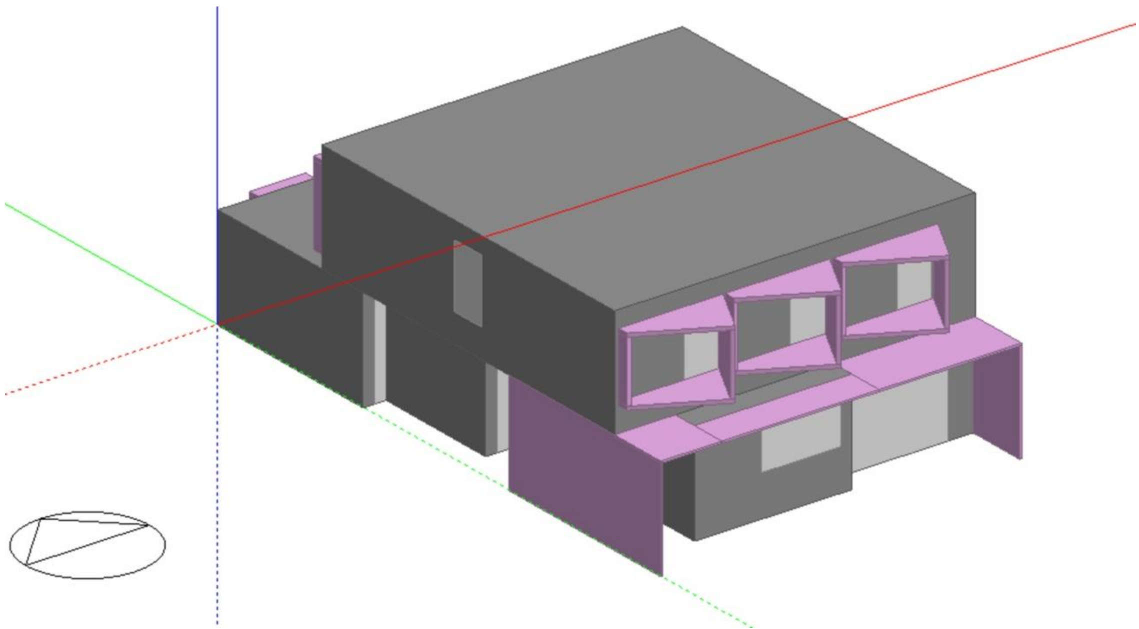

Figure 9. Model of the house in Design Builder.

The schematic diagram of the air conditioning system and the aerothermal system, as well as solar thermal panels to produce ACS, were also introduced into Design Builder. To adjust the simulation parameters to the real data, or to calibrate the model, they were compared with indoor air temperature and surface temperature values that had been obtained through monitoring. The monitoring system was designed using a wireless system. Temperature sensors were connected to small analysers (“EL-WiFi-TC. Thermocouple Probe Data logger”). The “EL-WiFi-TH, temperature and humidity data logger” analysers, with built-in sensors of temperature and relative humidity, interpreted the recorded data and sent Wi-Fi signals to a "RouterOS" router, connected to a laptop [40]. By installing the software “EasyLog Wi-Fi Software”, the data was received and stored in the computer. The climate file, including external air temperatures, relative humidity, and solar radiation levels by means of a pyranometer throughout the complete one-year cycle was obtained for the house in Molina de Segura and was also introduced.

Figures 10–13 show Computational Fluid Dynamics (CFD) results obtained through the Design Builder tool for 1 August 2018 at 3 p.m. and 1 February 2019 at 9 am. The climate differences between summer and winter are remarkable. To perform the simulations, the summer period was established from 1 May to 30 November and the winter regime from 1 December to 30 April. This division was based on prior simulation results, with the resulting model calibrated according to data obtained by monitoring the complete one-year cycle [63].

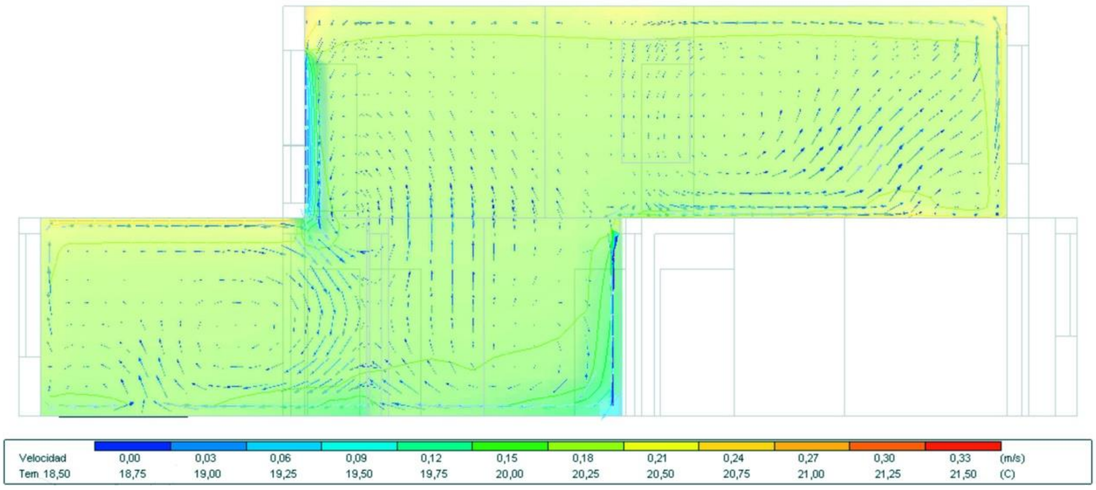

Figure 10. Simulated (CFD) of the house’s thermal behaviour; 1 February 2019, 9 am.

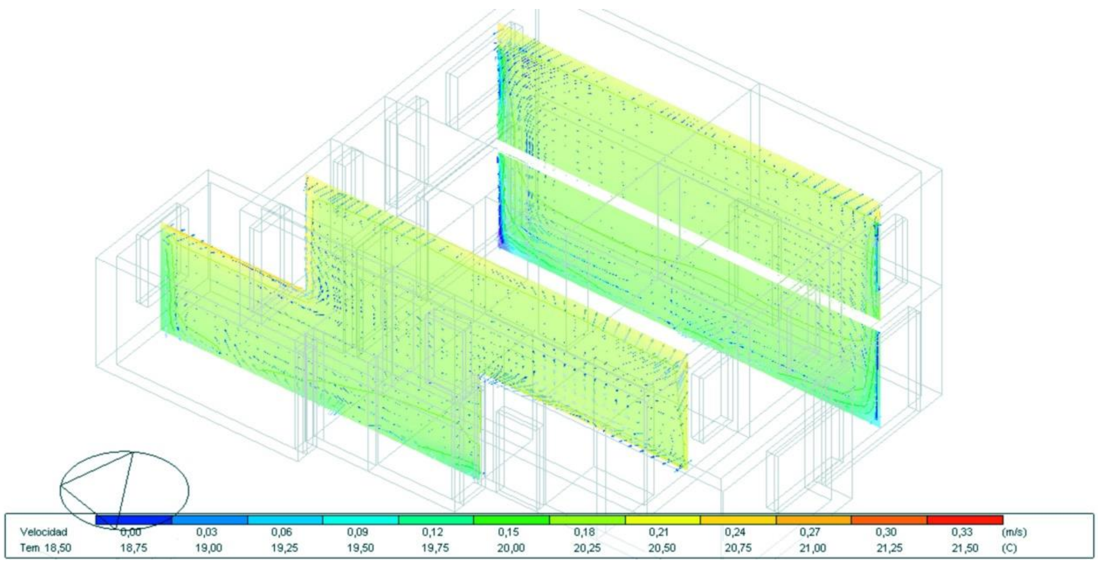

Figure 11. Simulated (CFD) of the house’s thermal behaviour; 1 February 2019, 9 am.

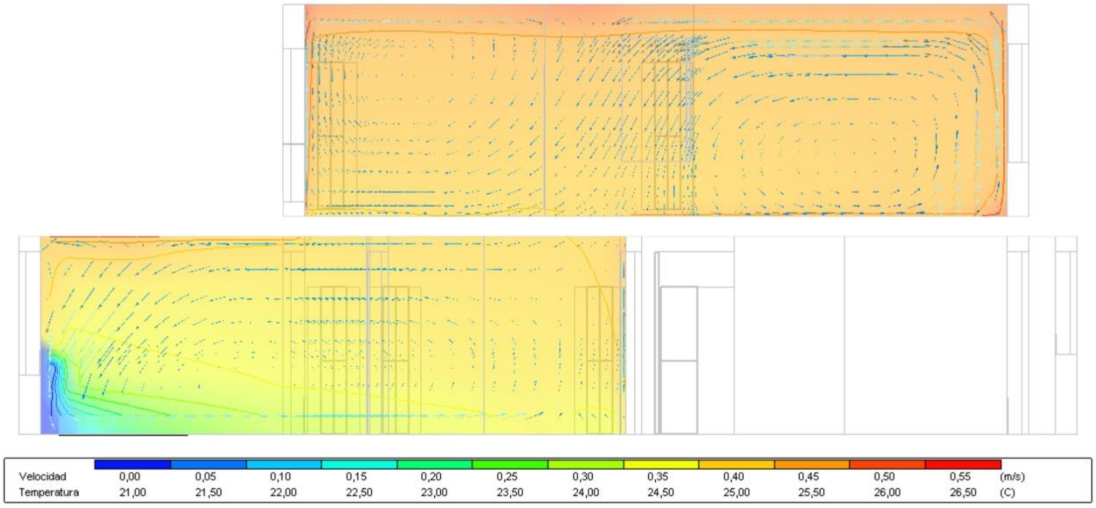

Figure 12. Simulated (CFD) of the house's thermal behaviour; 1 August 2018, 3 pm.

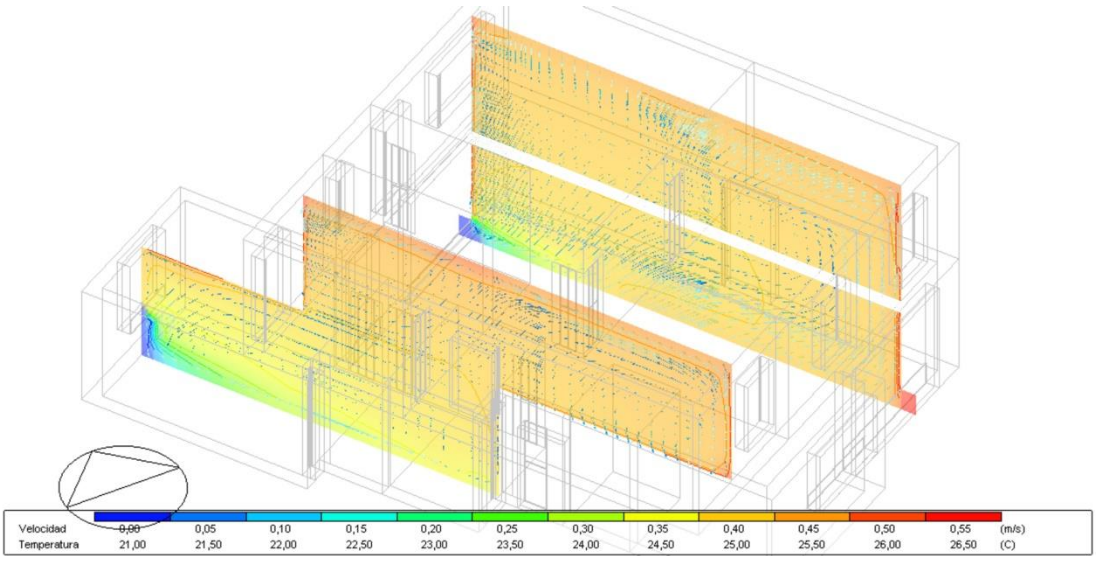

Figure 13. Simulated (CFD) of the house's thermal behaviour; 1 August 2018, 3 pm.

Based on the Design Builder simulations, impact results on annual energy demand were obtained for each housing type enclosure (Table 6). The climate file obtained in situ, by monitoring, was applied to obtain more accurate simulation results. Heat flows through the window openings accounted for almost 60% of the energy demand due to enclosure transmittance and 15% of the annual energy demand.

If we compare these results with those obtained for conventional housing constructions in the area (Table 7), the annual energy demand reduction is reduced by 39%, a high value that is mainly due to the breakage of thermal bridges and the increase in thickness of thermal insulation; 14.8 cm instead of the usual 4–6 cm [64]. The usual impact values of thermal bridges in conventional houses account for 3%–5% of the energy loss through the enclosure, while in the case of the house under study, this figure was reduced to 0.5% [65]. Simply by improving the enclosures' thermal insulation and thermal bridges, the application of the PH standard to the constructions on the Spanish Murcia-Alicante Mediterranean coast would bring about annual energy demand reductions of around 5 to 8 kWh/m^{2}year. This represents between 10% to 14% annual energy savings and this latter percentage would increase in the case of buildings built before the enforcement of the CTE.

Table 6. Energetic impact values of the different types of enclosures.

	Surface m^2	*U* Value W/m^2K	Annual Energy kWh/yr	Annual Energy Demand Impact kWh/m^2yr	Percentage %
Façade enclosure	181.79	0.2075	363.72	2.11	18.55
Window gap	40.09	2.91	1,124.07	6.49	57.31
Roof	173.20	0.2081	348.13	2.01	17.75
Contact with the ground	158.30	0.325	125.39	0.724	6.39
TOTAL	553.38		1,961.32	11.324	100

Table 7. Energetic impact values of the different types of enclosures.

	Passivhaus House		Standard House 1979–2006		Standard House 2006–2019	
	U Value W/m^2K	Annual Energy Demand Impact kWh/m^2yr	*U* Value W/m^2K	Annual Energy Demand Impact kWh/m^2yr	*U* Value W/m^2K	Annual Energy Demand Impact kWh/m^2yr
Opaque	0.221	2.11	0.476	4.67	0.421	4.32
Glazing	2.932	6.49	3.520	7.85	3.450	7.21
Roof	0.210	2.01	0.508	4.93	0.458	4.19
Ground	0.307	0.724	0.485	1.27	0.465	0.98
TOTAL		11.324		18.72		16.71

4.2. Energetic Impact of Air Infiltration

The energetic impact of air infiltration was obtained by applying the methodology described in Section 3.3. The values obtained are shown in Table 8. These values were also obtained in the Design Builder tool, once the value obtained in the Blower Door test was entered in the model and calibrated using the Persily–Kronvall estimate [59]. The table shows the values of the impact on annual energy demand of the air infiltration through the envelope, which alters the interior air temperature and its specific humidity [66]. The results for other conventional houses built in the same area have also been introduced. The energy impact percentages obtained are significant.

Table 8. Energetic impact values of the different types of enclosures.

	Passivhaus House	Standard House 1979–2006	Percentage	Standard House 2006–2019	Percentage
Test BD n_{50}	0.49	6.23		3.56	
Q_s (kWh/m^2yr)	1.377	9.543		4.971	
Q_l (kWh/m^2yr)	4.016	27.837		14.553	
Q_t (kWh/m^2yr)	5.393	37.379	14.43%	19.524	27.62%

The energy losses due to the air infiltration in the PH house analysed were between 5 and 7 times lower, leading to significant reductions in the percentage of impact on annual energy demand. The annual energy demand was reduced between 14 and 32 kWh/m^2yr, in percentage terms that is between 72.38% and 85.57%. This represents a major percentage drop compared to the conventional houses on the Mediterranean Murcia-Alicante coast.

4.3. Impact of Improvements of Thermal Transmittances and Air Infiltration on Annual Energy Demand

Once the results of thermal transmission (4.1) and air infiltration (4.2) were analysed, we could lay them out in a table together with the energy demand values for summer, winter, and a year, obtained from the Design Builder tool, for each of the three types studied (Table 9).

Table 9. Comparison of the energy impact in relation to the annual energy demands of the three housing types analysed.

	PH House	Percentage	House Type 1979–2006	Percentage	House Type 2006–2019	Percentage
Energy demand in summer (kWh/m^{2}yr)	14.321		50.64		42.29	
Energy demand in winter (kWh/m^{2}yr)	12.126		35.19		29.88	
Annual energy demand (kWh/m^{2}yr)	26.447	30.81%	85.83	100%	66.57	77.56%
Energy losses through *U* transmission (kWh/m^{2}yr)	11.324	42.82%	18.72	21.81%	16.71	25.10%
Energy losses through infiltration Q_t (kWh/m^{2}yr)	5.393	20.39%	37.379	43.05%	19.524	29.33%

Most notably, the annual energy demand of the PH house accounted for 30.81% of the usual value for buildings in the Mediterranean region under study. Regarding the most recent buildings built under the CTE umbrella, this percentage is 39.73% [57]. A drastic drop in energy consumption can be observed. The energy losses due to enclosure transmittance and air infiltration in the PH house were much lower, i.e., between 21.5 and 46 kWh m^{2}yr. They represent major annual energy demand drops for conventional housing on the Mediterranean Murcia-Alicante coast. The energy losses by infiltration were also found to be around 30%–40% of conventional housing energy demands, while this value was reduced to 20% in the case of the PH.

If we consider the values obtained in other studies, according to which the average impact of air infiltration on annual energy demand is around 12 kWh/m^{2}yr for Alicante, 10 kWh/m^{2}yr for Malaga, or 17 kWh/m^{2}yr for Barcelona [61], we can conclude that by applying the PH standard and its technical construction requirements, annual energy demand due to infiltration could be reduced by between 100% and 300%.

5. Conclusions

Quantifying the energetic impact of thermal transmission through enclosures and air infiltration is decisive to adapt the Passivhaus standard to the Spanish Mediterranean region. When gaps and glazing are designed to protect against solar radiation, overheating of indoor air and interior surfaces can be avoided, making it easier to implement the standard. This design layout leads to significant reductions in annual energy demand. Very thick thermal insulation could thus be applied to the envelope, which would work very well in winter, with energy demands below 15 kWh/m^{2}year and optimal comfort conditions with a well-designed air conditioning system in summer. The annual energy demand would not be too high, below 30 kW/m^{2}yr, a much lower value than the usual standards. Heat recovery systems relating to air renewal in summer, combined with the VRV system's air dehumidification, allow us to conclude the implementation of the standard could be generalised in the area, with low energy consumption. Low air infiltration implies low dehumidification system consumption, maintaining 50% of RH.

Highly satisfactory energy savings were obtained for the PH house under study, as follows:

- Energy losses through enclosure transmittance were 11.324 kWh/m^{2}yr, between 32% and 40% lower than those obtained in the usual homes in the region;
- Losses due to air infiltration were very low, of 5.393 kWh/m^{2}yr, given that the Blower Door test produced a very low n_{50} value of 0.49 ACH. They were between 5 and 7 times lower than in conventional homes in the area;
- The annual energy demand of PH housing was 69.19% below the usual value for buildings in the Mediterranean region. Regarding the most recent buildings built under the CTE umbrella, the reduction was 60.27%.

In future studies, investments necessary to build the house will be quantified and compared to conventional Murcia-Alicante coast standards. The energy saving values obtained in this study will be applied and the investments' amortisation period will be calculated. It will be possible to demonstrate the adequacy of the Passivhaus standard to the Administrations and the necessary corrections to apply the standard under the Spanish Mediterranean region climate. Policies proposing incentives to implement these construction systems and specific installations would undoubtedly lead to significant energy savings and thus reduce the environmental impacts deriving from the building and use of residential developments.

Author Contributions: Conceptualisation, methodology, measurements of *U*-value and test Blower Door, V.E.-I.; investigation, writing—original draft preparation, V.E.-I.; control of the data collecting of the monitorisation system and graphics, C.S.-S.; simulations by Design Builder, A.E.-F.; calibration of the model in Design Builder, and interpretation of data results, V.E.-I.; energetic impact of air infiltration, R.P.-G. and V.E.-I.

Funding: This research has been funded by the Vicerectorate of Campus Facilities & Techonology of the Universidad de Alicante, ref. 2018 34406P0002 P102 68000 (VIGROB 223).

Acknowledgments: Our thanks to the company "Habitar Natural 100 por 100 madera S.L." for their help in this study and to Jorge Vera Morales, promoter of the work, for having allowed us to access the house, monitor it, and take measurements. Our gratitude to Joaquín Ruiz Piñera, architect, designer, and director of the work, and Asier Elorza Echebarría, director of execution of the work, for their help in technical aspects.

Conflicts of Interest: The authors declare no conflict of interest.

References

1. European Commission. Directive 2002/91/EC of the European Parliament andof the Council of 16 December 2002 on the energy performance of buildings. *Off. J. Eur. Commun.* **2003**, *L1*, 65–70.
2. European Commission. Directive 2010/31/EU of European Parliament and ofthe Council of 19 May 2010 on the energy performance of buildings (recast). *Off. J. Eur. Union* **2010**, *L153*, 13–35.
3. Attia, S.; Eleftheriou, P.; Xeni, F.; Morlot, R.; Ménézo, C.; Kostopoulos, V.; Betsi, M.; Kalaitzoglou, I.; Pagliano, L.; Cellura, M.; et al. Overview and future challenges of nearly zero energy buildings (nZEB) design in Southern Europe. *Energy Build.* **2017**, *155*, 439–458. [CrossRef]
4. European Commission. Directive 2012/27/EU of European Parliament and of the Council of 25 October 2012 on energy efficiency, amending Directives2009/125/EC and 2010/30/EU and repealing Directives 2004/8/EC and2006/32/EC. *Off. J. Eur. Union* **2012**, *L315*, 1–56.
5. Technical Building Code CTE. *Basic Document on Energy Savings DB-HE*; Spanish Ministry of Housing: Madrid, Spain, 2006. (In Spanish)
6. *Orden VIV/984/2009, de 15 de abril, por la que se modifican determinados documentos básicos del Código Técnico de la Edificación aprobados por el Real Decreto 314/2006, de 17 de marzo, y el Real Decreto 1371/2007, de 19 de octubre*; Spanish Ministry of Housing: Madrid, Spain, 2009. (In Spanish)
7. *Orden FOM/1635/2013, de 10 de septiembre, por la que se actualiza el Documento Básico DB-HE Ahorro de Energía, del Código Técnico de la Edificación, aprobado por Real Decreto 314/2006, de 17 de marzo; (Publicado en: «BOE» núm. 219, de 12 de septiembre de 2013, páginas 67137–67209)*; Spanish Ministry of Public Works and Transport: Madrid, Spain, 2013. (In Spanish)
8. Passive House —Passivhaus Institut (PHI). Available online: http://passivehousecom/02informations/01whatisapassivehouse/01whatisapassivehousehtm (accessed on 9 April 2019).
9. Consoli, A.; Costanzo, V.; Evola, G.; Marletta, L. Refurbishing an existing apartment block in Mediterranean climate: Towards the Passivhaus standard. *Energy Procedia* **2017**, *111*, 397–406. [CrossRef]
10. Taleb, H.M. Using passive cooling strategies to improve thermal performance and reduce energy consumption of residential buildings in U.A.E. buildings. *Front. Arch. Res.* **2014**, *3*, 154–165. [CrossRef]
11. Schnieders, J.A.; Hermelink, A. CEPHEUS results: Measurements and occupants' satisfaction provide evidence for Passive Houses being an option for sustainable building. *Energy Policy* **2006**, *34*, 151–171. [CrossRef]
12. Costanzo, V.; Fabbri, K.; Piraccini, S. Stressing the passive behavior of a Passivhaus: An evidence-based scenario analysis for a Mediterranean case study. *Build. Environ.* **2018**, *142*, 265–277. [CrossRef]
13. Intelligent Energy Europe, Passive-On Project: Towards Passive Homes. 2007. Available online: http://dx.doi.org/10.1017/CBO9781107415324.004 (accessed on 11 April 2019).

14. Koller, C.; Talmon-Gros, M.J.; Junge, R.; Schuetze, T. Energy Toolbox—Framework for the Development of a Tool for the Primary Design of Zero Emission Buildings in European and Asian Cities. *Sustainability* **2017**, *9*, 2244. [CrossRef]
15. MED-ENEC. *Energy Efficiency in the Construction Sector in the Mediterranean*; MED-ENEC: Cairo, Egipt, 2011; Available online: http://www.med-enec.com (accessed on 18 April 2019).
16. IEEA. The Passivehaus Standard in European Warm Climates, EC Funded Project: Marketable Passive Homes for Winter and Summer Comfort. 2007. Available online: http://www.eerg.it/passive-on.org/CD/1.%20Technical%20Guidelines/Part%203/Part%203.pdf (accessed on 17 April 2019).
17. Algerian Ministry of Energy and Mines. Renewable Energy and Energy Efficiency Algerian Program. *Renew. Sustain. Energy Rev.* **2011**, *13*, 1584–1591.
18. Schnieders, J. Passive Houses in South West Europe: A Quantitative Investigation of Some Passive and Active Space Conditioning Techniques for Highly Energy Efficient Dwellings in the South West European. Region. Dissertation, Technical University Kaiserslautern, Kaiserslautern, Germany, 2009.
19. Figueiredo, A.; Figueira, J.; Vicente, R.; Maio, R. Thermal comfort and energy performance: Sensitivity analysis to apply the Passive House concept to the Portuguese climate. *Build. Environ.* **2016**, *103*, 276–288. [CrossRef]
20. Schnieders, J.; Wolfgang Feist, W.; Rongen, L. Passive Houses for different climate zones. *Energy Build.* **2015**, *105*, 71–87. [CrossRef]
21. EN 15251. *Indoor Environmental Input Parameters for Design and Assessment of Energy Performance of Buildings Addressing Indoor Air Quality, Thermal Environment, Lighting and Acoustic*; European Committee for Standardization: Brussels, Belgium, 2008.
22. Suárez, I.; Prieto, M.M.; Salgado, I. Dynamic evaluation of the thermal inertia of a single-family house: Scope of the retrofitting requirements to comply with Spanish regulations. *Energy Build.* **2017**, *153*, 209–218.
23. Pesic, N.; Roset Calzada, J.; Muros Alcojor, A. Natural ventilation potential of the Mediterranean coastal region of Catalonia. *Energy Build.* **2018**, *169*, 236–244. [CrossRef]
24. Fokaides, P.A.; Christoforou, E.; Ilic, M.; Papadopoulos, A. Performance of a Passive House under subtropical climatic conditions. *Energy Build.* **2016**, *133*, 14–31. [CrossRef]
25. Ali-Toudert, F.; Weidhaus, J. Numerical assessment and optimization of a low-energy residential building for Mediterranean and Saharan climates using a pilot project in Algeria. *Renew. Energy* **2017**, *101*, 327–346. [CrossRef]
26. Altan, H.; Gasperini, N.; Moshaver, S.; Frattari, A. Redesigning Terraced Social Housing in the UK for Flexibility Using Building Energy Simulation with Consideration of Passive Design. *Sustainability* **2015**, *7*, 5488–5507. [CrossRef]
27. Mihai, M.; Tanasiev, V.; Dinca, C.; Badea, A.; Vidu, R. Passive house analysis in terms of energy performance. *Energy Build.* **2017**, *144*, 74–86. [CrossRef]
28. Harkouss, F.; Fardoun, F.; Biwole, P.H. Passive design optimization of low energy buildings in different climates. *Energy* **2018**, *165*, 591–613. [CrossRef]
29. Dan, D.; Tanasa, C.; Stoian, V.; Brata, S.; Stoian, D.; Nagy Gyorgy, T.; Florut, S.C. Passive house design—An efficient solution for residential buildings in Romania. *Energy Sustain. Dev.* **2016**, *32*, 99–109. [CrossRef]
30. Design Builder. *Design Builder EnergyPlus Simulation Documentation for Design Builder v. 4.5.*; Design Builder Sortware Ltd.: Stroud, UK, 2015.
31. Mlakar, J.; Strancar, J. Overheating in residential passive house: solution strategies revealed and confirmed through data analysis and simulations. *Energy Build.* **2011**, *43*, 1443–1451. [CrossRef]
32. Presidencia de Gobierno. *Real Decreto 2429/1979, de 6 de julio, por el que se Aprueba la Norma Básica de Edificación NBE-CT-79, sobre Condiciones Térmicas en los Edificios*; Boletín Oficial del Estado: Madrid, Spain, 1979; Volume 253, pp. 24524–24550.
33. Bruno, R.; Bevilacqua, P.; Cuconati, T.; Arcuri, N. Energy evaluations of an innovative multi-storey wooden near Zero Energy Building designed for Mediterranean areas. *Appl. Energy* **2019**, *238*, 929–941. [CrossRef]
34. Kottek, M.; Grieser, J.; Beck, C.; Rudolf, B.; Rubel, F. World Map of the Köppen-Geiger climate classification updated. *Meteorol. Z.* **2006**, *15*, 259–263. [CrossRef]
35. ure(2017). World Map of the Köppen-Geiger Climate Classification Updated. High Resolution Map and Data (Version March 2017). KMZ File for Google Earth (High Res): Global_1986-2010_KG_5m.kmz.

Climate Change & Infectious Diseases. Available online: http://koeppen-geiger.vu-wien.ac.at (accessed on 13 April 2019).
36. Echarri, V.; Espinosa, A.; Rizo, C. Thermal Transmission through Existing Building Enclosures: Destructive Monitoring in Intermediate Layers versus Non-Destructive Monitoring with Sensors on Surfaces. *Sensors* **2017**, *17*, 2848. [CrossRef] [PubMed]
37. Dong, M.N.; Lu, Z.; Mo, T.Z.; Yang, J.Y.; Leng, Y.F.; Yang, L.L. Quantitative analysis on the effect of thermal bridges on energy consumption of residential buildings in hot summer and cold winter region. *J. Chongqing Jianzhu Univ.* **2008**, *30*, 5–8.
38. Garay, R.; Uriarte, A.; Apraiz, I. Performance assessment of thermal bridge elements into a full scale experimental study of a building façade. *Energy Build.* **2014**, *85*, 579–591. [CrossRef]
39. Wang, S.; Chen, Y. A simple procedure for calculating thermal response factors and conduction transfer functions of multilayer walls. *Appl. Therm. Eng.* **2002**, *22*, 333–338. [CrossRef]
40. Echarri Iribarren, V.; Galiano Garrigós, A.L.; González Avilés, A.B. Ceramics and healthy heating and cooling systems: Thermal ceramic panels in buildings. Conditions of comfort and energy demand versus convective systems. *Informes de la Construcción* **2016**, *68*, 19–32.
41. ISO. 13786:2007. Thermal Performance of Building Components. Dynamic Thermal Characteristics. Calculation Methods. Available online: https://www.iso.org/standard/40892.html (accessed on 19 September 2018).
42. Aznar, F.; Echarri, V.; Rizo, C.; Rizo, R. Modelling the Thermal Behaviour of a Building Facade Using Deep Learning. *PLoS ONE* **2018**, *13*, e0207616. [CrossRef]
43. CTE. Código Técnico de la Edificación. R/D 314/2006, de 17 de Marzo. Available online: http://www.codigotecnico.org/images/stories/pdf/realDecreto/RD3142006.pdf (accessed on 9 September 2017).
44. UNE EN ISO. 10456:2012. Materiales y Productos Para la Edificación. Propiedades Higrotérmicas. Valores Tabulados de Diseño y Procedimientos Para la Determinación de los Valores Térmicos Declarados y de Diseño. 2012. Available online: http://www.aenor.es/aenor/normas/normas/fichanorma.asp?tipo=N&codigo=N0049362#.Wgbq4tThCmw (accessed on 9 October 2017).
45. International Organization for Standardization. *Building Components and Building Elements. Thermal Resistance and Thermal Transmittance. Calculation Method*; ISO Standard 6946; International Organization for Standardization: Geneva, Switzerland, 2007; Available online: https://www.iso.org/obp/ui/#iso:std:iso:6946:ed-2:v1:en (accessed on 13 April 2019).
46. Evangelisti, L.; Battista, G.; Guattari, C.; Basilicata, C.; de Lieto Vollaro, R. Influence of the thermal inertia in the European simplified procedures for the assessment of buildings' energy performance. *Sustainability* **2014**, *6*, 4514–4524. [CrossRef]
47. HULC. Herramienta unificada Lider-Calener. Orden FOM/1635/2013, de 10 de septiembre (BOE de 12 de septiembre), por la que se actualiza el Documento Básico DB HE «Ahorro de Energía», del CTE. Available online: https://www.codigotecnico.org/index.php/menu-recursos/menu-aplicaciones/282-herramientaunificada-lider-calener.html (accessed on 9 September 2017).
48. Andújar Márquez, J.M.; Martínez Bohórquez, M.A.; Gómez Melgar, S. A New Metre for Cheap, Quick, Reliable and Simple Thermal Transmittance (U-Value) Measurements in Buildings. *Sensors* **2017**, *17*. [CrossRef] [PubMed]
49. Deconinck, A.H.; Roels, S. Comparison of characterisation methods determining the thermal resistance of building components from onsite measurements. *Energy Build.* **2016**, *130*, 309–320. [CrossRef]
50. ISO. 9869-1:2014. *Thermal Insulation-Building Elements-In Situ Measurement of Thermal Resistance and Thermal Transmittance. Part 1.: Heat Flow Meter Method*; ISO: Geneva, Switzerland, 2014; Available online: https://www.iso.org/standard/59697.html (accessed on 13 April 2019).
51. Gaspar, K.; Casals, M.; Gangolells, M. A comparison of standardized calculation methods for in situ measurements of façades U-value. *Energy Build.* **2016**, *130*, 592–599. [CrossRef]
52. Albatici, R.; Tonelli, A.M.; Chiogna, M. A comprehensive experimental approach for the validation of quantitative infrared thermography in the evaluation of building thermal transmittance. *Appl. Energy* **2015**, *141*, 218–228. [CrossRef]
53. Tinti, A.; Tarzia, A.; Passaro, A.; Angiuli, R. Thermographic analysis of polyurethane foams integrated with phase change materials designed for dynamic thermal insulation in refrigerated transport. *Appl. Therm. Eng.* **2014**, *70*, 201–210. [CrossRef]

54. Theodosiou, T.G.; Tsikaloudaki, A.G.; Kontoleon, K.J.; Bikas, D.K. Thermal bridging analysis on cladding systems for building facades. *Energy Build.* **2015**, *109*, 377–384. [CrossRef]
55. Feijó-Muñoz, J.; Poza-Casado, I.; González-Lezcano, R.A.; Pardal, C.; Echarri, V.; Assiego de Larriva, R.; Fernández-Agüera, J.; Dios-Viéitez, M.J.; del Campo-Díaz, V.J.; Montesdeoca Calderín, M.; et al. Methodology for the study of the envelope airtightness of residential buildings in Spain: A case study. *Energies* **2018**, *11*, 704. [CrossRef]
56. Bienvenido-Huertas, D.; Fernández Quiñones, J.A.; Moyano, J.; Rodríguez-Jiménez, C.E. Patents Analysis of Thermal Bridges in Slab Fronts and Their Effect on Energy Demand. *Energies* **2018**, *11*, 2222. [CrossRef]
57. Echarri-Iribarren, V.; Rizo-Maestre, C.; Echarri-Iribarren, F. Healthy Climate and Energy Savings: Using Termal Ceramic Panels and Solar Thermal Panels in Mediterranean Housing Blocks. *Energies* **2018**, *11*, 2707. [CrossRef]
58. Younes, C.; Shdid, C.A.; Bitsuamlak, G. Air infiltration through building envelopes: a review. *J. Build. Phys.* **2012**, *35*, 267–302. [CrossRef]
59. Sherman, M.H. Estimation of infiltration from leakage and climate indicators. *Energy Build.* **1987**, *10*, 81–86. [CrossRef]
60. Echarri, V. Thermal Ceramic Panels and Passive Systems in Mediterranean Housing: Energy Savings and Environmental Impacts. *Sustainability* **2017**, *9*, 1613. [CrossRef]
61. Feijó-Muñoz, J.; Pardal, C.; Echarri, V.; Fernández-Agüera, J.; Assiego de Larriva, R.; Montesdeoca Calderín, M.; Poza-Casado, I.; Padilla-Marcos, M.A.; Meiss, A. Energy impact of the air infiltration in residential buildings in the Mediterranean area of Spain and the Canary islands. *Energy Build.* **2019**, *188–189*, 226–238. [CrossRef]
62. Bienvenido-Huertas, D.; Moyano, J.; Rodríguez-Jiménez, C.E.; Marín, D. Applying an artificial neural network to assess thermal transmittance in walls by means of the thermometric method. *Appl. Energy* **2019**, *233–234*, 1–14. [CrossRef]
63. Echarri-Iribarren, V.; Rizo-Maestre, C.; Sanjuan-Palermo, J.L. Underfloor Heating Using Ceramic Thermal Panels and Solar Thermal Panels in Public Buildings in the Mediterranean: Energy Savings and Healthy Indoor Environment. *Appl. Sci.* **2019**, *9*, 2089. [CrossRef]
64. Šadauskiene, J.; Ramanauskas, J.; Šeduikyte, L.; Daukšys, M.; Vasylius, A. A Simplified Methodology for Evaluating the Impact of Point Thermal Bridges on the High-Energy Performance of a Passive House. *Sustainability* **2015**, *7*, 16687–16702. [CrossRef]
65. Fu, X.; Qian, X.; Wang, L. Energy Efficiency for Airtightness and Exterior Wall Insulation of Passive Houses in Hot Summer and Cold Winter Zone of China. *Sustainability* **2017**, *9*, 1097. [CrossRef]
66. Johnston, D.; Siddall, M. The Building Fabric Thermal Performance of Passivhaus Dwellings—Does It Do What It Says on the Tin? *Sustainability* **2016**, *8*, 97. [CrossRef]